Effect of potassium-chromate and sodium-nitrite on concrete steel-rebar degradation in sulphate and saline media

Joshua Olusegun Okeniyi [a,*], Olugbenga Adeshola Omotosho [a], Oluseyi Olanrewaju Ajayi [a], Cleophas Akintoye Loto [a,b]

[a] Mechanical Engineering Department, Covenant University, P.M.B.1023, Ota, Nigeria
[b] Chemical and Metallurgical Engineering Department, Tshwane University of Technology, Pretoria, South Africa

HIGHLIGHTS

- 0.145 M K_2CrO_4 inhibitor admixture exhibited optimal performance in H_2SO_4 medium.
- 0.679 M $NaNO_2$ inhibitor admixture exhibited optimal performance in NaCl medium.
- $NaNO_2$ inhibitor admixture exhibited poor corrosion inhibition performance in H_2SO_4.
- Compressive tests showed that H_2SO_4 had adverse effect on the strength of concrete.
- Compressive tests showed that NaCl had no adverse effect on concrete strength.

ARTICLE INFO

ABSTRACT

In this paper, effect of potassium-chromate (K_2CrO_4) and sodium-nitrite ($NaNO_2$) on concrete steel-rebar degradation in sulphuric-acid and in sodium-chloride media were studied. Electrochemical monitoring of open circuit potential and compressive strength effect of the different concentrations of these admixtures in steel-reinforced concretes immersed in the acidic/marine-simulating environments were analysed for detailing admixture performance. Results subjected to ASTM C876 interpretations showed that concrete admixed with 0.145 M potassium-chromate exhibited optimum inhibition effectiveness with good compressive strength improvement in the acidic medium. In the saline medium, the concrete admixed with 0.679 M sodium-nitrite exhibited optimal inhibition performance, but with reduction in concrete compressive strength.

1. Introduction

Corrosion induced degradation of steel reinforcement (steel-rebar) in concrete is the major cause of deterioration of concrete structures including building facilities, bridges, parking garages and other civil infrastructures [1–3]. Industrial, coastal and marine environments of the world are well dispersed with rust stained, cracked and spalled concrete structures caused by this form of degradation of the reinforcing steel and the composite constituents of the concrete structures [2,4,5]. The environments in which these structures exist provide more than adequate agents necessary for initiating and propagating the corrosion failure process. These corrosion inducing agents include oxygen, carbon dioxide and moisture from the atmosphere [5], sulphate ions from microbial or sewage environment [2,6] and chloride ions from saline or marine environment [1,4,7,8]. This is such that the corrosion destruction of concrete steel-rebar has contributed more than 80% of all the damages of reinforced concrete structures globally [9]. Consequent repair, maintenance and rehabilitation, to ensure in-service continuance and durability, of concrete infrastructures gulp substantial resources of intensive labour and escalating costs annually [3,5,10]. This, coupled with the inevitability of steel-reinforced concrete as the material of choice for various construction works in modern society [10–12], necessitates needs of research activities aimed towards corrosion prevention for the durability of concrete facilities [13].

Several methods could be used for the protection of steel-reinforced concrete structures from corrosion degradation. Some of the

* Corresponding author. Tel.: +234 8069836502.
E-mail addresses: joshua.okeniyi@covenantuniversity.edu.ng, josoken@yahoo.com (J.O. Okeniyi).

methods include: paintings, coatings or waterproofing membranes of the outer surface of the concrete structure [9,14–16]; coating of the steel rebar [17]; cathodic protection of steel rebar [18]; and corrosion inhibitors admixed in concrete [19,20]. While each of these methods had been employed in studies with varying degrees of success, the use of corrosion inhibitor admixtures had been described to be an effective method, which combines the advantages of lower cost with easy application compared to other methods, for controlling concrete steel-rebar corrosion [19,21].

Corrosion inhibitor is a chemical substance which, in the presence of corrosive agent, decreases the corrosion rate in a corroding system when used at suitable concentration [21–23]. Several studies have investigated the inhibiting effectiveness and the compressive strength effect of different corrosion inhibitor admixtures in reinforced concrete [3,9,22,24–27]. Many of these studies linked the repressive capabilities to corrosion degradation and the strength properties of the reinforced concrete due to the applied inhibitors studied to the inhibitor types and their admixed concentration. Not many studies, however, had been carried out on potassium-chromate and sodium-nitrite and their synergies as well as the effect of their admixture in concrete on the compressive strength of the concrete structures. Also, there is dearth of work using the statistical tools, either of the normal probability density function (PDF) or the Weibull PDF to analyse electrochemical potential readings, which could be attended with fluctuations that could make interpretation from such readings difficult.

The focus of this study is to comparatively investigate the effect of potassium-chromate and sodium-nitrite as inhibitors on the corrosion degradation of steel-rebar in concrete. The corrosion monitoring technique of the half-cell (or open circuit) potential [22,24–26] was employed in the work, in accordance with ASTM C876-91 R99 [28], to study the performance of the different concentrations of the two inhibitors and their synergies in sulphuric-acid and sodium-chloride media. The statistical modelling tools of the Normal PDF and the Weibull PDF were used to analyse the quality, uniformity and reliability of the comparative effectiveness of each inhibitor concentrations and goodness-of-fit criteria, by the PDF's, were determined using Kolmogorov–Smirnov statistics [29,30]. Also, the effect of the different concentrations of inhibitor admixtures on the compressive strengths of the concrete specimens were investigated and reported.

2. Materials and methods

2.1. Concrete blocks preparation

Schematic drawings and pictorial representations of the materials and experimental set-up employed for this study are shown in Fig. 1. Each concrete block, Fig. 1(a), used for the experiment was made using Portland cement, sand and gravel mixed with water at a mix ratio of 1:2:4 (cement, sand and gravel). The formulation used for each reinforced concrete specimen was (in kg/m^3): cement 320, water 140, sand 700 and gravel 1150. The water/cement (w/c) ratio was 0.44.

Thirty concrete blocks were used for the electrochemical monitoring experiment; these were set-up in two-sets of fifteen specimens. Each block was admixed with different concentrations of inhibitors and a fixed amount of 0.1 M NaCl to accelerate the corrosion of the embedded steel by providing increased chloride ions in the matrix and particularly around the steel-rebar. The inhibitor admixtures ranged from 1.5 g to 9.0 g by mass in increments of 1.5 g for each of the potassium-chromate and sodium-nitrite inhibitors. In concentration terms, these were: 0.048 M, 0.097 M, 0.145 M, 0.193 M, 0.242 M and 0.290 M of potassium-chromate; and 0.136 M, 0.272 M, 0.408 M, 0.544 M, 0.679 M and 0.815 M of sodium-nitrite. The synergetic combinations were: concrete admixed with 1.5 g (0.048 M) potassium-chromate and 3.0 g (0.272 M) sodium-nitrite; and concrete admixed with 3.0 g (0.097 M) potassium-chromate and 1.5 g (0.136 M) sodium-nitrite. All chemicals used were of AnalaR reagent grade.

DIN-ST 60 mm type of steel rebar was used for the reinforcement. The steel was obtained from Oshogbo Steel Rolling Mill, Nigeria and its chemical composition include: 0.3%C, 0.25%Si, 1.5%Mn, 0.04%P, 0.64%S, 0.25%Cu, 0.1%Cr, 0.11%Ni, and the remainder Fe. The rebar were cut into several pieces each with a length of 160 mm and 10 mm diameter and embedded in the concrete. Abrasive grinder

was used to remove the mill scales and rust stains on the steel specimens before each was placed in its concrete block. The protruded end of the block was painted to prevent atmospheric corrosion.

2.2. Experimental procedures

The first sets of fifteen steel-reinforced concrete specimens were partially immersed in plastic bowls containing 0.5 M dilute sulphuric-acid (H$_2$SO$_4$) medium to simulate microbial (or sewage) environments. The second sets were partially immersed in plastic bowls containing 3.5% sodium-chloride (NaCl) medium to simulate marine/saline environments. In each of these plastic bowls, the corrosive test-media were made up to just below the steel reinforcement but without making contact with it, as was schematically shown in Fig. 1(b).

Open circuit potential (OCP) readings were measured by placing a Cu/CuSO$_4$ electrode (CSE), Model 8-A (Tinker & Rasor®), firmly on a conducting sponge, that was wetted with electrical contact solution as prescribed by ASTM C876-91 R99 [28,30–33] before being placed on the concrete block, Fig. 1(c). The contact solution was prepared with potable water to which local detergent and isopropyl alcohol was added as described in ASTM C876-91 R04. The COM input (negative) socket of a high impedance digital multimeter was connected to the Cu/CuSO$_4$ electrode while the red lead terminal (the V input and positive socket) was connected to the exposed part of the embedded steel reinforcement to make a complete electrical circuit. The Model MY64 multimeter that was employed for the corrosion potential measurement was obtained from MASTECH® (China), Fig. 1(d). This MY64 multimeter model had input impedance of 10 Ω, accuracy of ±(0.5% reading +2 digits) and was operated with 9 V battery of type 6F22; and by these the instrument conforms to the specifications of ASTM C876-91 R99 [28] for open circuit potential measuring apparatus. These and other technical/accuracy specifications of the MY64 multimeter model, by the manufacturer, were shown in Fig. 1(e).

OCP for each specimen was monitored over an exposure period of 32 days. The readings were taken at three different points on each concrete block directly over the embedded steel reinforcement [20,22] in 2-day intervals for the exposure period. The average of the three readings was computed and this was subjected to data analysis and interpretation based on ASTM C876-91 R99 [28,30–33].

2.3. Data analysis

The distribution functions used for analysing open circuit potential readings include the Normal distribution, whose cumulative density function (CDF), F_N, could be represented by [34–36]:

$$F_N(x) = \frac{1}{\sigma\sqrt{2\pi}} \int_{-\infty}^{x} \exp\left[-\left(\frac{x-\mu}{2\sigma^2}\right)^2\right] dx \tag{1}$$

where μ is the mean and σ is the standard deviation of the sample variable x. The other distribution function includes the two-parameter Weibull distribution with CDF, F_W, given by [35,37–39]:

$$F_W(x) = 1 - \exp\left(-\left(\frac{x}{c}\right)^k\right) \tag{2}$$

where k is the shape parameter and c is the characteristic value or the scale parameter of the Weibull distribution function. Eq. (2) can be expressed in linear form [37–40] to obtain

$$\ln[-\ln[1 - F_W(x)]] = k\ln x - k\ln c \tag{3}$$

A threshold value $x_0 = 0$ had been assumed by using the two-parameter Weibull [39]. In order to ensure the consistencies of the negative OCP values, especially, with the logarithmic nature of Eq. (3), x values had been taken to be in negative millivolts versus Cu/CuSO$_4$ electrode, i.e. $-mV$ (CSE). This approach finds similarity with the data presentation approach of [22]. Hence, positive values of x are used in the equations for the distribution functions. To model the quality and variability of the measured data using the Weibull distribution, estimations of the Weibull mean μ_W and standard deviation σ_W were obtained from [37–41]

$$\mu_W = c\Gamma\left(1 + \frac{1}{k}\right) \tag{4}$$

$$\sigma_W = \sqrt{c^2\left\{\Gamma\left(1 + \frac{2}{k}\right) - \left[\Gamma\left(1 + \frac{1}{k}\right)\right]^2\right\}} \tag{5}$$

where $\Gamma(\cdot)$ is the gamma function of $(\cdot)$.

2.4. Goodness-of-fit test statistics

To ascertain the compatibility of the OCP data to each of the Normal and the Weibull distributions, the Kolmogorov–Smirnov (K–S) goodness-of-fit test (GoF) statistics [29,34,36–39,41–45] was used. This measures the absolute difference between empirical distribution function $F^*(x)$ and theoretical distribution function $F(x)$ through the statistics [29,36,38,41,42]
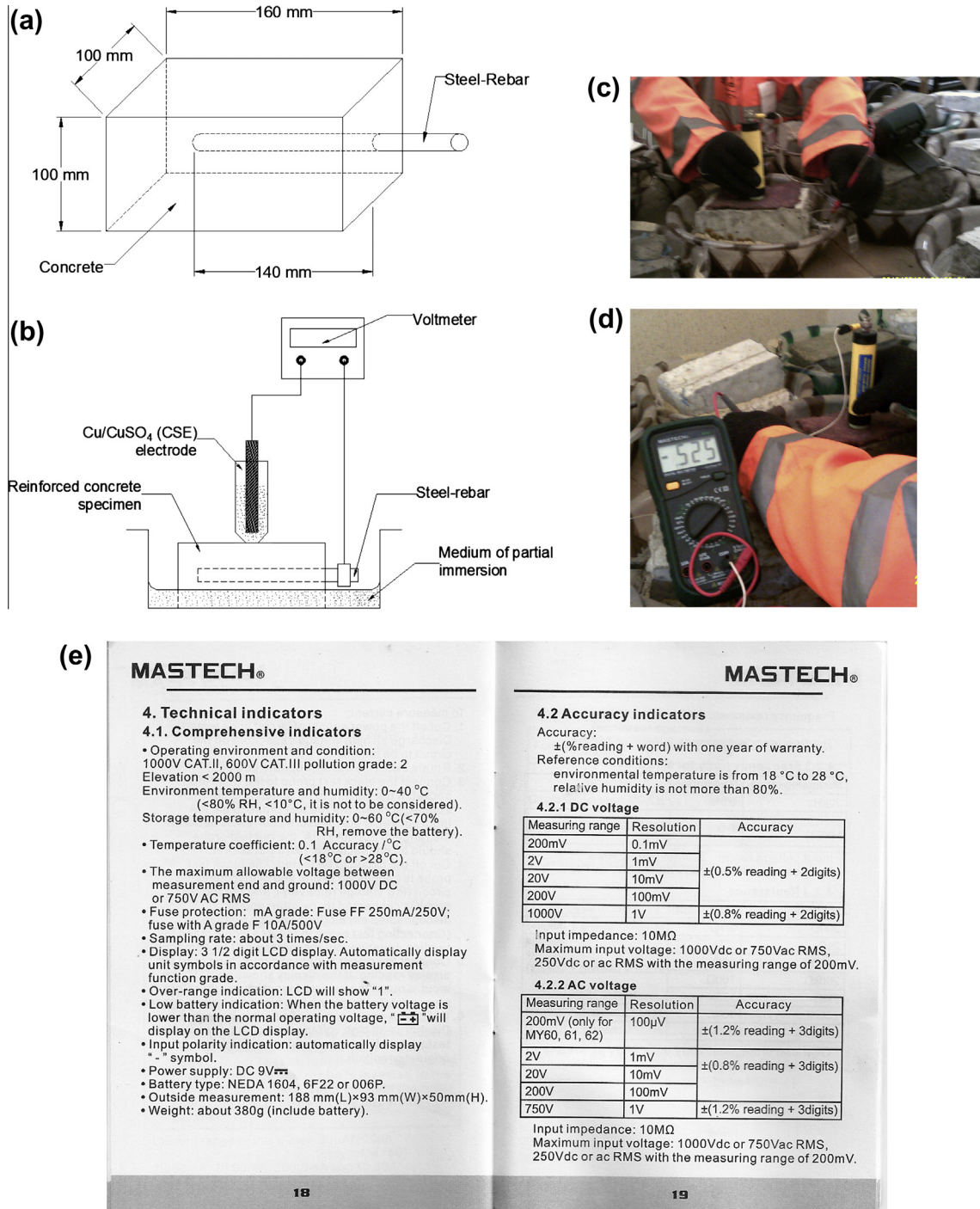
Fig. 1. Materials and set-up of electrochemical, half-cell (or open circuit) potential, monitoring experiment (a) schematic dimension of steel-reinforced concrete specimen, (b) schematic set-up of potential measurement, (c) measuring corrosion potential, (d) readout example of corrosion potential, and (e) manufacturer's technical and accuracy specifications of voltmeter instrument, MASTECH® equipment, showing conformity with specifications of ASTM C876-91 R99.

$$d = d(x_1, \ldots, x_n) = \sqrt{n} \sup_{-\infty < x < \infty} |F * (x) - F(x)| \tag{6}$$

where n is the sample size. By employing the method described in [29], the value of d computed from Eq. (6) was used with n to directly compute the one-sample two-sided probabilistic value (p-value) that the OCP data follow each distribution function studied. These p-value computations not only establish, or otherwise, how well the measured OCP data followed the distribution functions but also facilitate direct comparisons of the description of the OCP data by the Normal and the Weibull distribution functions.

2.5. Compressive strength determination for specimen samples

The consistency of the different concentrations of potassium-chromate and sodium-nitrite on the steel-reinforced concrete specimens was determined by investigating the compressive strength of the concrete samples after the potential monitoring period [3,22]. This was done by removing each specimen from their respective test medium, allowing it to dry/harden in air for seven days after which each concrete block was carefully placed lengthwise on a compressive fracture machine and load applied until the block failed. Compressive failure loads from these

were then compared with that from two other steel-reinforced concrete specimens, without inhibitor admixture, one of which was cured in air and the other cured in water for two weeks [24].

3. Results and discussions

3.1. Experimental results

Graphical plots of averaged readings of open circuit potential (OCP) against time, obtained during the experiment for the two-set specimens of reinforced concrete samples are presented in Fig. 2 for the two media – Fig. 2(a) for H_2SO_4 and Fig. 2(b) for NaCl.

The open circuit potential readings from the graphical plots shown in Fig. 2(a) and (b) could be observed as being predominated with fluctuations in the form of spikes of varying amplitudes for each concentration of inhibitors presented. Studies referred to these sharp oscillatory drifts between the active and passive regions as "electrochemical noise" [46,47]. The fluctuating spikes can be attributed to constant corrosion damage of the protective film by the notorious corrosive media and subsequent inhibition by the constantly formed protective layer of applied inhibitor admixture on the reinforcing steel [46]. Interpreting inhibiting effectiveness by the varying concentrations of admixed inhibitor using these fluctuations in the observed data was difficult. These difficulties of performance interpretations were however tackled by the use of probabilistic modelling tools for analysing and estimating effectiveness of each inhibitor concentration in the corrosive media.

Fig. 2. Graphical plots of open circuit potential readings vs. time for steel-reinforced concrete samples with varying concentrations of potassium-chromate and sodium-nitrite admixtures (a) samples in H_2SO_4 medium; (b) samples in NaCl medium.

3.2. Statistical probability modelling

The probability density function (PDF) plots for the Normal and Weibull distribution functions are presented Fig. 3 for the reinforced concrete samples. Results of analytical modelling of the mean OCP data using the Normal distribution and the Weibull distribution fittings are presented in Table 1 for reinforced concrete samples with admixed inhibitors immersed in sulphuric-acid medium, while those immersed in sodium-chloride medium are presented in Table 2.

Table 1 shows that the analysed results of the experimental OCP data obtained from the concrete samples immersed in H_2SO_4 medium had considerable discrepancies in the estimated parameters by the Normal, compared to the estimations by the Weibull distribution. These discrepancies can also be inferred from the PDF plots of the two distributions in H_2SO_4 medium presented in Fig. 3(a) and (b). Both the Weibull mean (μ_W) and standard deviation (σ_W) were well overestimated than that obtained from the sample mean (μ) and standard deviation (σ) for each of the H_2SO_4-immersed samples. Also, the Weibull mean modelling were at larger values of Weibull probability of Weibull mean (Prob(μ_W)) than the Weibull probability of sample mean (Prob(μ)). Weibull PDF modelled data of seven specimens of concrete samples in H_2SO_4 medium, out of the fifteen considered, did not follow the Weibull distribution function because their K–S p-values are less than the level of significance, $\alpha = 0.05$, usually employed in studies. The remaining eight specimens immersed in H_2SO_4 medium follow the Weibull PDF according to the K–S GoF criteria.

Eleven specimens of concrete samples immersed in H_2SO_4 medium follow the Normal PDF with K–S p-values greater than 0.05. These include four out of the seven specimens which did not follow the Weibull distribution function. Also, the control specimen in H_2SO_4 medium, which follows the Weibull PDF with a Weibull model K–S p-value of 0.0575, did not follow the Normal PDF at which its modelled K–S p-value is 0.0268, a value less than 0.05.

From Fig. 3(c) and (d) and Table 2, analysed results of the OCP data by the two-parameter Weibull distribution function compare very well with that by the Normal distribution function, for all the reinforced concrete samples immersed in NaCl medium. Estimated parameters from the two distribution models exhibited equalities of inhibiting qualities, i.e. $\mu \approx \mu_W$, to two correct to decimal places for all the samples in NaCl medium. Also, the p-values from the Kolmogorov–Smirnov (K–S) goodness-of-fit test show that the measured OCP data, for all these NaCl-immersed concrete samples, follow both the Normal and the two-parameter Weibull distribution functions. These p-values were all greater than 0.05. Also, the large shape parameter (k) values of the Weibull model of these samples imply small scatter of OCP data, which thus translate to good uniformity of the measured data.

By the foregoing considerations, three specimens of concrete samples have their analysed OCP data following neither the Normal PDF nor the Weibull PDF in this study. These three specimens include concrete samples, immersed in H_2SO_4, which are admixed respectively with 9.0 g $NaNO_2$ inhibitor, 7.5 g $NaNO_2$ inhibitor and 4.5 g $NaNO_2$ inhibitor. The concrete sample admixed with 9.0 g $NaNO_2$ inhibitor in H_2SO_4 medium was characterised by the lowest shape factor (k) value of 0.91 in this study, followed by the sample admixed with 7.5 g $NaNO_2$ inhibitor in H_2SO_4 medium which has a k value of 0.98. These shape factor (k) values represent the Weibull slope of the modelled data. The fact that these shape factor values are less than unity indicates large scatter of the modelled OCP data even as it also suggests low measure of uniformity in the modelled data of the specimen samples. The third concrete sample admixed with 4.5 g $NaNO_2$ inhibitor in H_2SO_4 medium had a larger shape factor (k) value of 1.93. While the reason for the data from this sample not following the Weibull would require further analytical
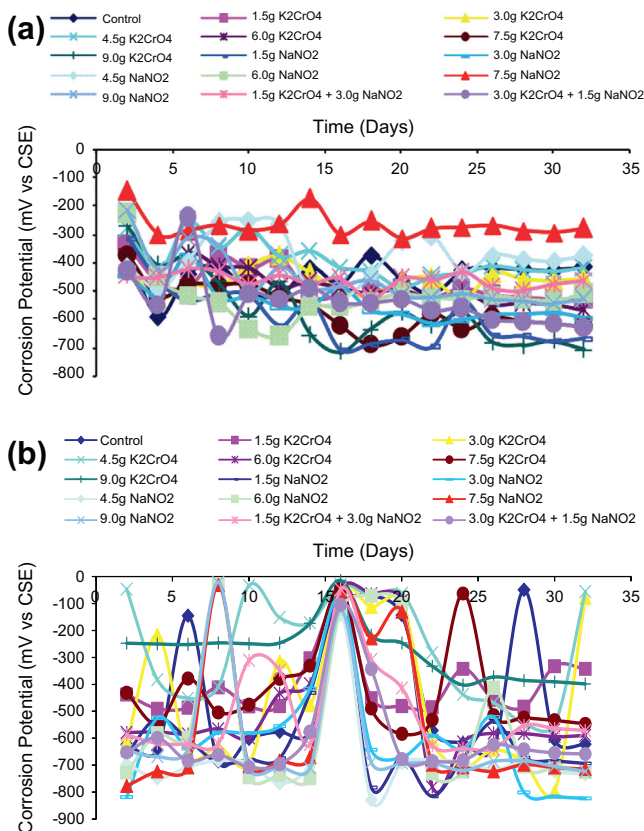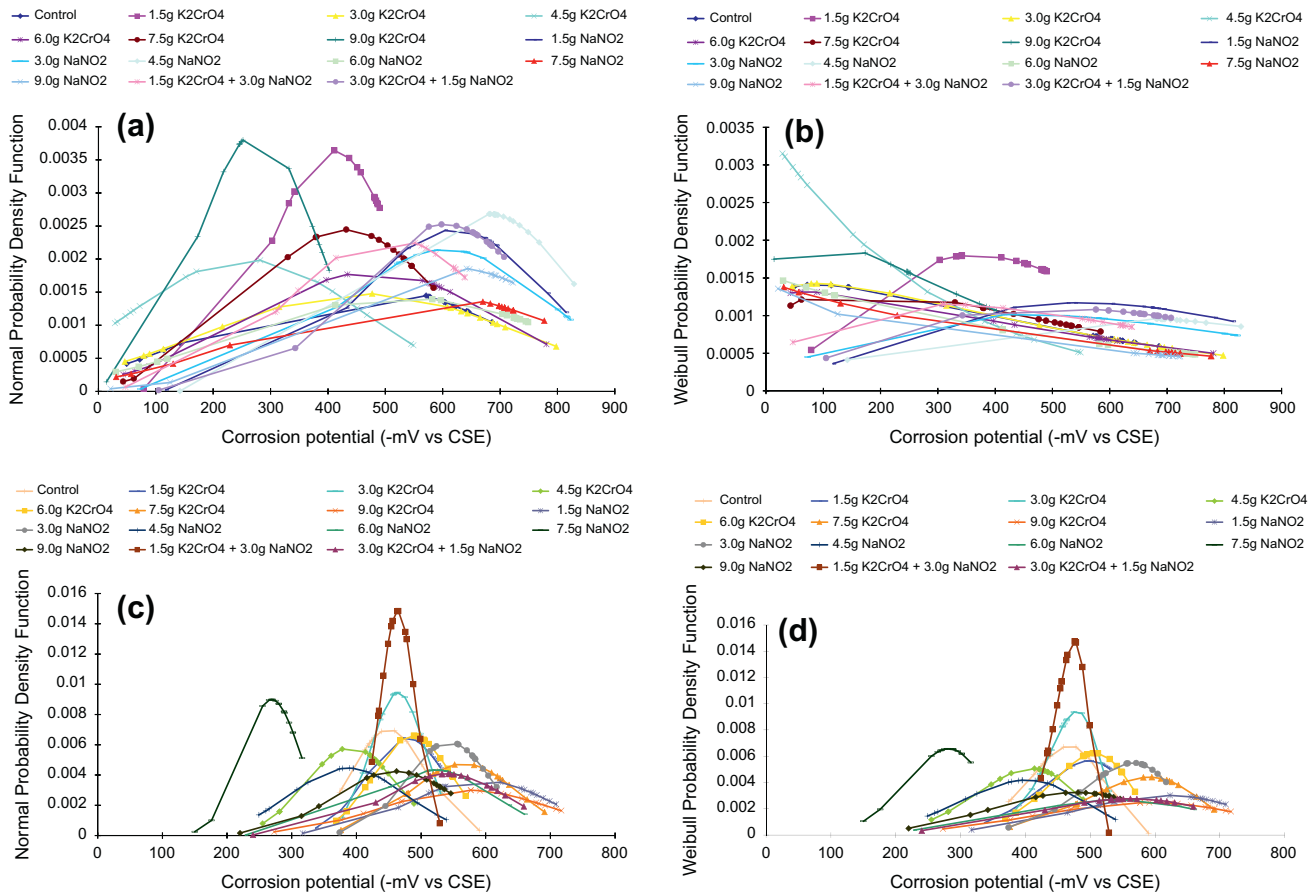
Fig. 3. Probability density function (PDF) plots for steel-reinforced concrete samples (a) Normal PDF for H_2SO_4-immersed samples; (b) Weibull PDF for H_2SO_4-immersed samples; (c) Normal PDF for NaCl-immersed samples; (d) Weibull PDF for NaCl-immersed samples.

Table 1
Estimated parameters from the Normal and Weibull distribution analyses of the open circuit potential readings for steel-reinforced concrete samples in H_2SO_4 medium.

S/No	Admixed inhibitor	Normal distribution			Weibull distribution						
		μ ($-mV$ (CSE))	σ	p-value (K–S)	k	c	μ_W ($-mV$ (CSE))	σ_W	Prob(μ_W)	Prob(μ)	p-Value (K–S)
1	Control	455.69	247.07	0.0268	1.14	553.00	527.96	465.07	0.6127	0.5517	0.0575
2	1.5 g K_2CrO_4	409.06	109.48	0.3699	2.11	494.23	437.72	217.61	0.5386	0.4885	0.0225
3	3.0 g K_2CrO_4	461.69	269.52	0.1979	1.14	545.37	520.09	456.46	0.6122	0.5625	0.3164
4	4.5 g K_2CrO_4	258.94	199.91	0.5611	1.01	283.94	282.88	280.36	0.6307	0.5980	0.6913
5	6.0 g K_2CrO_4	479.50	220.96	0.0516	1.10	611.59	589.47	534.75	0.6172	0.5344	0.1030
6	7.5 g K_2CrO_4	429.69	163.12	0.3334	1.25	555.68	517.20	415.16	0.5991	0.5154	0.0444
7	9.0 g K_2CrO_4	276.31	102.08	0.4324	1.17	373.28	353.41	302.73	0.6086	0.5049	0.0540
8	1.5 g $NaNO_2$	619.75	163.23	0.1624	2.08	752.26	666.32	336.41	0.5403	0.4875	0.0982
9	3.0 g $NaNO_2$	605.75	186.22	0.5473	1.66	760.92	679.98	419.83	0.5637	0.4955	0.0755
10	4.5 g $NaNO_2$	680.13	148.73	0.0041	1.93	854.12	757.54	408.60	0.5476	0.4748	0.0085
11	6.0 g $NaNO_2$	529.13	281.30	0.1225	1.00	657.74	659.04	662.11	0.6328	0.5530	0.0748
12	7.5 g $NaNO_2$	560.00	271.14	0.0098	0.98	723.07	729.38	744.18	0.6353	0.5409	0.0357
13	9.0 g $NaNO_2$	613.69	213.15	0.0057	0.91	898.80	937.47	1026.04	0.6463	0.5061	0.0040
14	1.5 g K_2CrO_4 + 3.0 g $NaNO_2$	505.63	171.33	0.1254	1.47	644.55	583.11	402.17	0.5780	0.5030	0.0235
15	3.0 g K_2CrO_4 + 1.5 g $NaNO_2$	602.88	158.01	0.0971	1.88	748.44	664.41	367.70	0.5505	0.4864	0.0099

scrutiny beyond the scope of this present study, it is opined that this could be due to the existence of outlier in the measured data. This could be such that the outlier, that seems not to affect the slope of the plot, however, affected how well the data for the sample followed the Weibull PDF fitting.

3.3. Corrosion condition classifications

The estimated sample mean, representing the Normal mean model, and the Weibull mean were subjected to the corrosion

classification standard of ASTM C876-91 R99 [28] with reference to Cu/CuSO$_4$ electrode [32,33]. The corrosion condition classifications, obtained based on the standard, are presented in Table 3 for concrete samples immersed in sulphuric-acid medium and in Table 4 for samples immersed in sodium-chloride medium.

It could be observed from Table 3 that the corrosion condition classifications, based on ASTM C876-91 R99 [28], of the Normal and Weibull estimates of inhibiting quality for concrete samples immersed in H_2SO_4 medium find agreements in ten out of the fifteen classified specimens. The remaining five samples were

Table 2
Normal and Weibull distribution modelling of the open circuit potential readings for steel-reinforced concrete samples in NaCl medium.

S/No	Admixed inhibitor	Normal distribution			Weibull distribution						
		μ (−mV (CSE))	σ	p-value (K–S)	k	c	μ_W (−mV (CSE))	σ_W	Prob(μ_W)	Prob(μ)	p-Value (K–S)
1	Control	450.19	56.86	0.5401	8.72	475.48	449.62	61.52	0.4588	0.4625	0.3556
2	1.5 g K$_2$CrO$_4$	477.19	61.70	0.1746	7.72	507.16	476.79	73.11	0.4624	0.4646	0.2919
3	3.0 g K$_2$CrO$_4$	464.25	42.27	0.9576	12.34	483.05	463.38	45.68	0.4505	0.4581	0.7503
4	4.5 g K$_2$CrO$_4$	391.56	68.38	0.2557	5.74	423.11	391.58	78.98	0.4732	0.4731	0.4830
5	6.0 g K$_2$CrO$_4$	486.88	60.43	0.5508	8.66	514.12	486.00	66.95	0.4590	0.4642	0.7801
6	7.5 g K$_2$CrO$_4$	565.69	83.90	0.9142	7.16	603.07	564.79	92.94	0.4649	0.4687	0.9902
7	9.0 g K$_2$CrO$_4$	571.19	133.12	0.5264	4.10	631.18	572.94	157.03	0.4894	0.4851	0.6315
8	1.5 g NaNO$_2$	592.38	108.73	0.4413	5.20	644.75	593.30	131.21	0.4775	0.4748	0.5814
9	3.0 g NaNO$_2$	543.06	64.55	0.5299	8.52	574.17	542.35	75.85	0.4595	0.4632	0.8201
10	4.5 g NaNO$_2$	386.75	89.54	0.9469	4.69	422.55	386.53	93.89	0.4824	0.4833	0.9778
11	6.0 g NaNO$_2$	521.81	92.25	0.0694	4.10	582.81	529.00	145.15	0.4894	0.4704	0.0847
12	7.5 g NaNO$_2$	268.88	44.38	0.1696	5.14	293.70	270.10	60.32	0.4780	0.4701	0.2359
13	9.0 g NaNO$_2$	459.75	93.86	0.4612	4.35	507.36	462.08	120.20	0.4862	0.4788	0.2599
14	1.5 g K$_2$CrO$_4$ + 3.0 g NaNO$_2$	464.13	26.88	0.9777	19.09	476.67	463.49	30.05	0.4432	0.4517	0.7991
15	3.0 g K$_2$CrO$_4$ + 1.5 g NaNO$_2$	539.38	97.94	0.4271	4.36	597.36	544.10	141.33	0.4862	0.4732	0.4167

Table 3
Corrosion condition classification models for concrete samples immersed in H$_2$SO$_4$ medium.

S/No	Admixed inhibitor	μ	Corrosion condition (normal PDF model)	μ_W	Corrosion condition (Weibull PDF model)
1	Control	455.69	High (>90% risk of corrosion)	527.96	Severe corrosion
2	1.5 g K$_2$CrO$_4$	409.06	High (>90% risk of corrosion)	437.72	High (>90% risk of corrosion)
3	3.0 g K$_2$CrO$_4$	461.69	High (>90% risk of corrosion)	520.09	Severe corrosion
4	4.5 g K$_2$CrO$_4$	258.94	Intermediate corrosion risk	282.88	Intermediate corrosion risk
5	6.0 g K$_2$CrO$_4$	479.5	High (>90% risk of corrosion)	589.47	Severe corrosion
6	7.5 g K$_2$CrO$_4$	429.69	High (>90% risk of corrosion)	517.2	Severe corrosion
7	9.0 g K$_2$CrO$_4$	276.31	Intermediate corrosion risk	353.41	High (>90% risk of corrosion)
8	1.5 g NaNO$_2$	619.75	Severe corrosion	666.32	Severe corrosion
9	3.0 g NaNO$_2$	605.75	Severe corrosion	679.98	Severe corrosion
10	4.5 g NaNO$_2$	680.13	Severe corrosion	757.54	Severe corrosion
11	6.0 g NaNO$_2$	529.13	Severe corrosion	659.04	Severe corrosion
12	7.5 g NaNO$_2$	560	Severe corrosion	729.38	Severe corrosion
13	9.0 g NaNO$_2$	613.69	Severe corrosion	937.47	Severe corrosion
14	1.5 g K$_2$CrO$_4$ + 3.0 g NaNO$_2$	505.63	Severe corrosion	583.11	Severe corrosion
15	3.0 g K$_2$CrO$_4$ + 1.5 g NaNO$_2$	602.88	Severe corrosion	664.41	Severe corrosion

Table 4
Corrosion condition classification models for concrete samples immersed in NaCl medium.

S/No	Admixed inhibitor	μ	Corrosion condition (Normal PDF Model)	μ_W	Corrosion condition (Weibull PDF model)
1	Control	450.19	High (>90% risk of corrosion)	449.62	High (>90% risk of corrosion)
2	1.5 g K$_2$CrO$_4$	477.19	High (>90% risk of corrosion)	476.79	High (>90% risk of Corrosion)
3	3.0 g K$_2$CrO$_4$	464.25	High (>90% risk of corrosion)	463.38	High (>90% risk of corrosion)
4	4.5 g K$_2$CrO$_4$	391.56	High (>90% risk of corrosion)	391.58	High (>90% risk of corrosion)
5	6.0 g K$_2$CrO$_4$	486.88	High (>90% risk of corrosion)	486	High (>90% risk of corrosion)
6	7.5 g K$_2$CrO$_4$	565.69	Severe corrosion	564.79	Severe corrosion
7	9.0 g K$_2$CrO$_4$	571.19	Severe corrosion	572.94	Severe corrosion
8	1.5 g NaNO$_2$	592.38	Severe corrosion	593.3	Severe corrosion
9	3.0 g NaNO$_2$	543.06	Severe corrosion	542.35	Severe corrosion
10	4.5 g NaNO$_2$	386.75	High (>90% risk of corrosion)	386.53	High (>90% risk of Corrosion)
11	6.0 g NaNO$_2$	521.81	Severe corrosion	529	Severe corrosion
12	7.5 g NaNO$_2$	268.88	Intermediate corrosion risk	270.1	Intermediate corrosion risk
13	9.0 g NaNO$_2$	459.75	High (>90% risk of corrosion)	462.08	High (>90% risk of corrosion)
14	1.5 g K$_2$CrO$_4$ + 3.0 g NaNO$_2$	464.13	High (>90% risk of corrosion)	463.49	High (>90% risk of corrosion)
15	3.0 g K$_2$CrO$_4$ + 1.5 g NaNO$_2$	539.38	Severe corrosion	544.1	Severe corrosion

classified as exhibiting higher probability of corrosion risk by the extreme value distribution model of the Weibull PDF than the classifications obtained from the Normal distribution model. From Table 4, however, the corrosion condition classifications of the Normal and Weibull estimates of inhibiting effect for concrete samples immersed in NaCl medium were in agreements for all the specimen samples studied.

3.4. Performance rankings of inhibiting effectiveness

Rankings of inhibiting performance by the Weibull, compared with the Normal, distribution function are presented in Fig. 4 for the specimens of steel-reinforced concrete samples immersed in H$_2$SO$_4$ medium, Fig. 4(a), and for the samples in NaCl medium, Fig. 4(b).
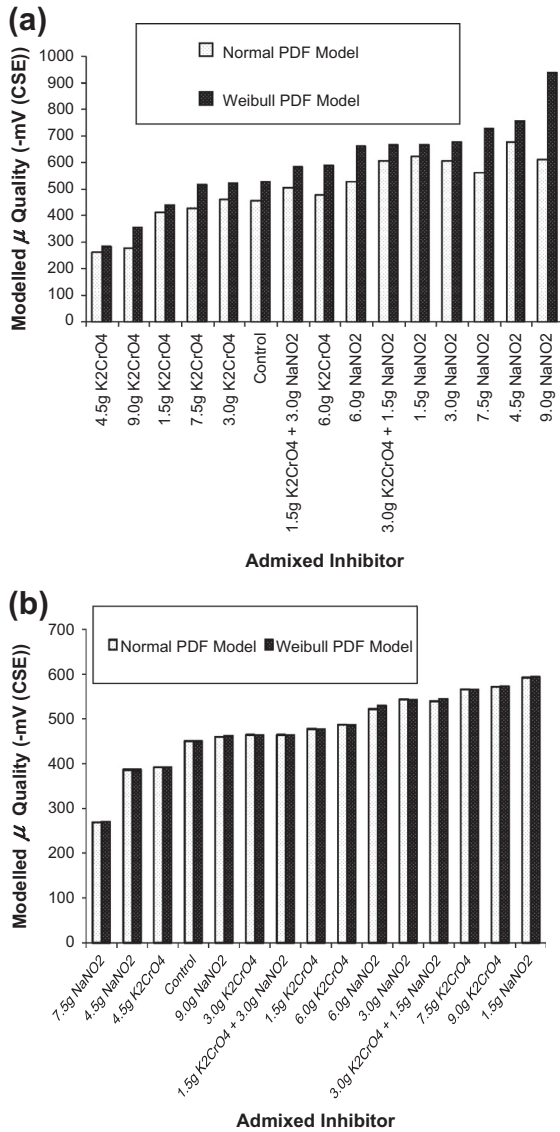
Fig. 4. Rankings of inhibiting performance for specimens of concrete samples by the Weibull, compared with the Normal, PDF (a) samples in H$_2$SO$_4$ medium; (b) samples in NaCl medium.

From the performance ranking in Fig. 4(a), the two-tier PDF models showed that most of the concentrations of potassium-chromate admixtures considered in this study exhibited better inhibiting quality than the control specimen in H$_2$SO$_4$ medium. These include 4.5 g K$_2$CrO$_4$, 9.0 g K$_2$CrO$_4$, 1.5 g K$_2$CrO$_4$, 7.5 g K$_2$CrO$_4$ and 3.0 g K$_2$CrO$_4$. Optimal inhibiting performance was exhibited by the modelled OCP data of 4.5 g K$_2$CrO$_4$ admixture in reinforced concrete, modelled at Normal PDF $\mu = -258.94$ mV (CSE); Weibull PDF $\mu = -282.88$ mV (CSE) at 63.07% reliability. This modelled performance of 4.5 g K$_2$CrO$_4$ admixture in H$_2$SO$_4$ medium was classified to be in the "intermediate corrosion risk" in Table 3 based on ASTM C876.

However, with the exception of 1.5 g K$_2$CrO$_4$ admixture, the Normal PDF rankings and classifications of the remaining potassium-chromate inhibitors that exhibited better performance than the control specimen differ from the model rankings by the Weibull PDF. As the only exception, both the Normal PDF model and the Weibull PDF model classified the concrete admixed with 1.5 g K$_2$CrO$_4$ to the "high (>90% risk of corrosion)" range (from Table 3). The Normal PDF modelled 9.0 g K$_2$CrO$_4$ admixture to

the "intermediate corrosion risk" range, but the Weibull PDF modelled this admixture sample to the "high (>90% risk of corrosion) range". Concrete admixtures with 7.5 g K$_2$CrO$_4$ and 3.0 g K$_2$CrO$_4$ were also classified by the Normal PDF to the "high (>90% risk of corrosion)" range but they were modelled for the "severe corrosion" range by the Weibull PDF.

All the concrete admixtures with sodium-nitrite concentrations were modelled as exhibiting very poor performance, in this study, compared to the control specimen in H$_2$SO$_4$ medium. Although the concrete samples with synergetic admixtures of potassium-chromate showed better performance than most of the concrete samples with sodium-nitrite alone, the inhibition performance of the synergies still lagged behind that of the control specimen in the H$_2$SO$_4$ medium.

The performance ranking in Fig. 4(b) showed that concrete sample admixed with 7.5 g NaNO$_2$ exhibited optimal inhibiting quality in sodium-chloride medium. This sample was modelled with inhibiting quality $\mu = -268.88$ mV (CSE) at a variability of 44.38 by the Normal PDF, Table 2, while by the Weibull PDF modelling, the inhibiting quality $\mu = -270.10$ mV (CSE). The reliability of the Weibull model for this inhibiting quality equals 47.80%. The Normal and Weibull distributions modelled the corrosion condition of this sample to the "intermediate corrosion risk" range, Table 4, according to ASTM standard C876-91 R99 [28].

Also identified, by the ranking in Fig. 4(b), as exhibiting good inhibiting effectiveness in NaCl medium, compared to the control specimen, include the concrete sample with 4.5 g NaNO$_2$ and the concrete sample with 4.5 g K$_2$CrO$_4$. For concrete sample with 4.5 g NaNO$_2$, Normal PDF $\mu = -386.75$ mV (CSE); Weibull PDF $\mu = -386.52$ mV (CSE) at 48.24% reliability. And for the concrete sample with 4.5 g K$_2$CrO$_4$ Normal PDF $\mu = -391.56$ mV (CSE); Weibull PDF $\mu = -391.58$ mV (CSE) at 47.32% reliability. Both of these samples were modelled to the "high (>90% risk of corrosion)" range by the two PDF models. All the other concentrations of admixed inhibitors, including the synergetic admixtures, in NaCl medium had inhibiting effectiveness which lagged behind that of the control sample in the medium.

3.5. Compressive strength effect of admixture on concrete

The compressive fracture loads of the steel-reinforced concrete samples were presented, in ranking order of the compressive strengths exhibited in their respective media, in Fig. 5. This figure showed that the compressive failure loads ranged from 256 kN to 294 kN for the concrete samples partially immersed in sulphuric-acid medium, Fig. 5(a), while it ranged from 269 kN to 330 kN for the samples immersed in sodium-chloride medium, Fig. 5(b). These failure loads of steel-reinforced concrete samples in both media surpassed that of the specimen cured in water which had compressive failure load of 210 kN. These higher-than water-cured specimen failure load values could be due to multiple reasons. The samples with inhibitor admixtures could have higher failure loads as a result of the relative chemical reaction hardening effect of the inhibitor substance with the concrete. Also, the experimental samples were partially immersed in their sulphate or saline media with the other halves exposed to the air throughout the monitoring period. By this, greater consistency could be infused in these samples, than that obtained in the water-cured specimen, through the dual hardening media of air and the solution of partial immersion.

Twelve out of the samples immersed in H$_2$SO$_4$ medium showed improvement in compressive strength compared to the control sample in the medium, Fig. 5(a). From these, concrete sample with the synergetic admixture of 1.5 g potassium-chromate and 3.0 g sodium-nitrite had the highest compressive strength improvement with the failure load of 294 kN followed by the sample with 3.0 g potassium-chromate which had 288 kN failure load. The control
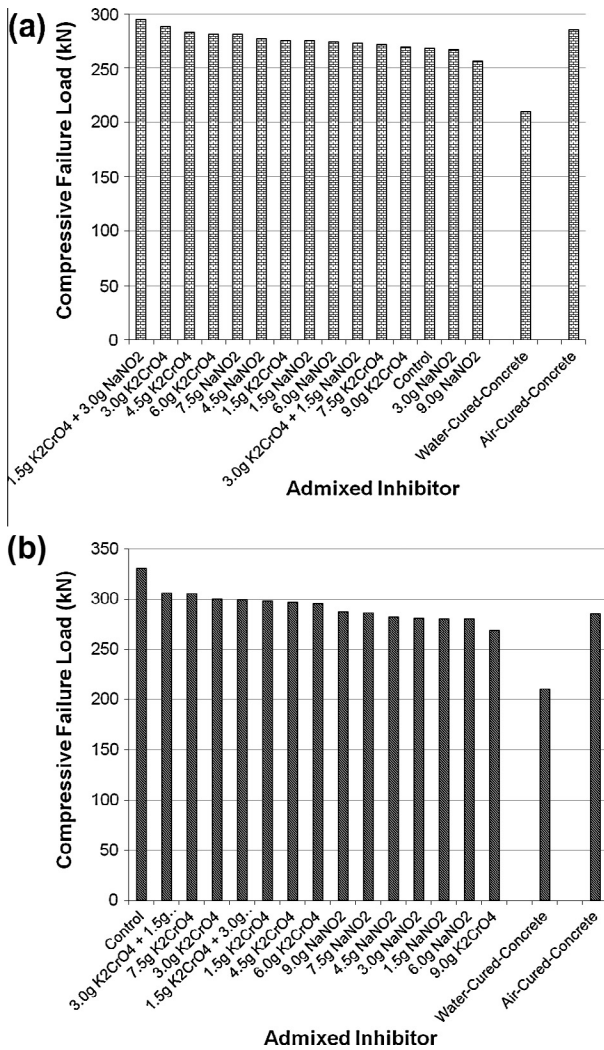
Fig. 5. Rankings of compressive failure load of steel-reinforced concrete samples with inhibitor admixtures and comparisons with that of water-cured and air-cured specimens (a) samples partially immersed in H_2SO_4 medium (b) samples partially immersed in NaCl medium.

achieved with the additional advantage of compressive strength improvement, of 283 kN, over the failure load (268 kN) of the control.

These types of inferences could not be drawn, in this study, for concrete samples partially immersed in NaCl medium. This is because the control sample which failed at the compressive load of 330 kN, had higher failure load than that of the specimen cured in air (285 kN) and the failure loads of all the concrete samples with inhibitor admixtures in the medium, Fig 4(b). The concrete sample with 3.0 g K_2CrO_4 and 1.5 g $NaNO_2$ synergistic admixture at its compressive failure load of 306 kN trailed behind the compressive strength of the control specimen though it surpassed that of the other samples with inhibitor admixtures. These bear suggestions that the NaCl medium had no adverse effect on the compressive strength of the concrete samples partially immersed in it and that all the inhibitor admixtures studied herein caused losses in the compressive strength of the concrete samples in the medium. Of all these, the greatest loss in compressive strength was exhibited by the concrete sample with 9.0 g K_2CrO_4 admixture, at its compressive failure load of 269 kN. These also implied that the optimal inhibiting quality exhibited by the concrete sample admixed with 7.5 g $NaNO_2$, at its failure load of 286 kN that is less than the 330 kN observed with control, was attained at the expense of the compressive strength of the concrete. However, these losses in compressive strength of concrete samples in NaCl medium were in relative comparison with that of the control sample in the medium. In other considerations, ten of the concrete samples with inhibitor admixtures, in the medium, also exhibited higher compressive failure loads than that of the specimen cured in air, just as the control sample, Fig. 5(b). This further suggests that the compressive strength improvement by the NaCl medium overshot the losses in compressive strengths that could be caused by these inhibitors. However, these foster recommendation of the requirement of further studies seeking for inhibitor admixtures for achieving both corrosion inhibition of concrete steel-rebar with the added advantage of better compressive strength improvement in the concrete than that of the control sample in the NaCl environment.

4. Conclusion

The effect of potassium-chromate and sodium-nitrite on concrete steel-rebar degradation in sulphuric-acid and sodium-chloride media had been investigated in this study. From the results in the study, the following conclusions can be drawn:

- In a modelling agreement by the Normal and the Weibull PDF, steel-reinforced concrete sample with 4.5 g K_2CrO_4 (0.145 M) inhibitor admixture was estimated as exhibiting the lowest probability of corrosion risk in sulphuric-acid medium. The corrosion condition for this inhibitor concentration classified to the "intermediate corrosion risk" range both by the Normal and the Weibull PDF as per ASTM C876.
- $NaNO_2$ admixtures performed poorly at inhibiting steel-rebar corrosion in the acidic medium.
- Steel-reinforced concrete sample with 7.5 g $NaNO_2$ (0.679 M) inhibitor admixture was estimated as exhibiting optimal performance in sodium-chloride medium by both statistical modelling distributions. The corrosion condition for this inhibitor concentration also classified to the "intermediate corrosion risk" range both by the Normal and the Weibull PDF as per ASTM C876.
- In this study, the 0.145 M K_2CrO_4 admixture combined optimal inhibition of steel-rebar corrosion with added advantage of compressive strength improvement that was better than that

sample which failed at 268 kN compressive load exhibited greater compressive strength improvement than concrete sample admixed with 3.0 g sodium-nitrite which failed at 267 kN and that with 9.0 g sodium-nitrite that failed at 256 kN. It is worth noting that all the concrete samples admixed with potassium-chromate inhibitors, though not in a particular order of concentration, exhibited greater compressive failure strength than the control sample in H_2SO_4 medium.

With the exception of concrete sample with 1.5 g K_2CrO_4 + 3.0 g $NaNO_2$ and that with 3.0 g K_2CrO_4, all the other concrete samples immersed in H_2SO_4 medium had compressive failure loads which fell short that of the concrete specimen cured in air, at its 285 kN failure load. That the control sample failed at a lower compressive load of 268 kN, than that of the specimen cured in air, indicated that the sulphuric-acid medium had adverse effect on the compressive strength of the concrete samples partially immersed in it. By this, it could be inferred that the adverse effect on the compressive strength of the concrete samples by this medium was improved by the twelve samples that failed at higher compressive loads than that of the control sample in the medium. These, therefore, bear implication that the optimum inhibiting quality exhibited by the concrete sample admixed with 4.5 g K_2CrO_4 was

of the control sample in concrete immersed in the H_2SO_4 environment.

- However, the optimal 0.679 M $NaNO_2$ admixture, in the NaCl medium, exhibited reduction in compressive strength in comparison with that of the control sample in the medium, that no other admixture studied attained the compressive strength of the control sample in the medium fosters recommendation for further studies in search of admixtures that will both inhibit steel-rebar corrosion and improve concrete compressive strength of in the NaCl medium.

References

[1] Junzhi Z, Jianze W, Deyu K. Chloride diffusivity analysis of existing concrete based on Fick's second law. J Wuhan Univ Technol – Mater Sci Ed 2010;25(1):142–6.
[2] Di Maio AA, Lima LJ, Traversa LP. Chloride profiles and diffusion coefficients in structures located in marine environment. Struct Concr 2004;5(1):1–4.
[3] Schutter GD, Luo L. Effect of corrosion inhibiting admixtures on concrete properties. Constr Build Mater 2004;18:483–9.
[4] Maruthamuthu S, Muthukumar N, Natesan M, Palaniswamy N. Role of air microbes on atmospheric corrosion. Curr Sci 2008;94(3):359–63.
[5] Lee C, Bonacci JF, Thomas MDA, Maalej M, Khajehpour S, Hearn N, et al. Accelerated corrosion and repair of reinforced concrete columns using carbon fibre reinforced polymer sheets. Can J Civ Eng 2000;27:941–8.
[6] Prasad J, Jain DK, Ahuja AK. Factors influencing the sulphate resistance of cement concrete and mortar. Asian J Civ Eng (Building and Housing) 2006;7(3):259–68.
[7] Abosrra L, Ashour AF, Youseffi M. Corrosion of steel reinforcement in concrete of different compressive strengths. Constr Build Mater 2011;25:3915–25.
[8] Pradhan B, Bhattacharjee B. Performance evaluation of rebar in chloride contaminated concrete by corrosion rate. Constr Build Mater 2009;23:2346–56.
[9] Francišković J, Mikšić B, Rogan I, Tomičić M. Protection and repair of reinforced concrete structures by means of Mci-Inhibitors and corrosion protective materials. In: Structural Engineering Conferences: International Conferences on Bridges, Dubrovnik, Croatia; 2006. p. 553−560.
[10] Akinyemi OO, Alamu OJ. Effect of 0.05 M NaCl on corrosion of coated reinforcing steels in concrete. The Pac J Sci Technol 2009;10(1):462–71.
[11] Shi X, Yang Z, Liu Y, Cross D. Strength and corrosion properties of Portland cement mortar and concrete with mineral admixtures. Constr Build Mater 2011;25:3245–56.
[12] Arum C, Olotuah AO. Making of strong and durable concrete. Emir J Eng Res 2006;11(1):25–31.
[13] Andrade C. Reinforcement corrosion: research needs. In: Alexander MG, Beushausen H-D, Dehn F, Moyo P, editors. Concrete repair, rehabilitation and retrofitting II. London: Taylor & Francis Group; 2009. p. 81–8.
[14] Aguiar JB, Camões A, Moreira PM. Performance of concrete in aggressive environment. Intern J Concr Struct Mater 2008;2(1):21–5.
[15] Rodrigues MPMC, Costa MRN, Mendes AM, Marques MIE. Effectiveness of surface coatings to protect reinforced concrete in marine environments. Mater Struct 2000;33(10):618–26.
[16] Gu GP, Beaudoin JJ. Cost-effective solutions for corrosion prevention and repair in concrete structures. Constr Can 1997;39(6):36–9.
[17] Kepler JL, Darwin D, Locke CE Jr. Evaluation of corrosion protection methods for reinforced concrete highway structures. SM Report No. 58. Lawrence, Kansas: University of Kansas Center for Research Inc; 2000.
[18] Sekar ASS, Saraswathy V, Parthiban GT. Cathodic protection of steel in concrete using conductive polymer overlays. Int J Electrochem Sci 2007;2(7):872–82.
[19] Hewayde E, Nehdi ML, Allouche E, Nakhla G. Using concrete admixtures for sulphuric acid resistance. Constr Mater 2007;160(CM1):25–35.
[20] Saraswathy V, Song H-W. Improving the durability of concrete by using inhibitors. Build Environ 2007;42:464–72.
[21] Söylev TA, Richardson MG. Corrosion inhibitors for steel in concrete: state-of-the-art report. Constr Build Mater 2008;22:609–22.
[22] Burubai W, Dagogo G. Comparative study of inhibitors on the corrosion of mild steel reinforcement in concrete. Agric Eng Intern: The CIGR Ejorunal Manuscript BC 06 008, Vol. IX; 2007.
[23] Revie RW, Uhlig HH. Corrosion and corrosion control. 4th ed. Hoboken New Jersey: John Wiley & Sons, Inc; 2008.
[24] Omotosho OA, Loto CA, Ajayi OO, Okeniyi JO. Aniline effect on concrete steel rebar degradation in saline and sulfate media. Agric Eng Int: CIGR Ejournal 2011;13(2).
[25] Al-Mehthel M, Al-Dulaijan S, Al-Idi SH, Shameem M, Ali MR, Maslehuddin M. Performance of generic and proprietary corrosion inhibitors in chloride-contaminated silica fume cement concrete. Constr Build Mater 2009;23:1768–74.
[26] Robertson IN, Newtson C. Performance of corrosion inhibitors in concrete exposed to marine environment. In: Alexander MG, Beushausen H-D, Dehn F, Moyo P, editors. Concrete repair, rehabilitation and retrofitting II. London: Taylor & Francis Group; 2009. p. 901–6.
[27] Holloway L, Nairn K, Forsyth M. Concentration monitoring and performance of a migratory corrosion inhibitor in steel-reinforced concrete. Cem Concr Res 2004;34:1435–40.
[28] ASTM C876-91 R99. Standard test method for half-cell potentials of uncoated reinforcing steel in concrete. ASTM International, West Conshohocken, PA.
[29] Okeniyi JO, Okeniyi ET. Implementation of Kolmogorov-Smirnov *p*-value computation in Visual Basic®: implication for Microsoft Excel® library function. J Statistical Comput Simul 2012;82(12):1727–41.
[30] Song H-W, Pack S-W, Ann KY. Probabilistic assessment to predict the time to corrosion of steel in reinforced concrete tunnel box exposed to sea water. Constr Build Mater 2009;23:3270–8.
[31] Gulikers J. Statistical interpretation of results of potential mapping on reinforced concrete structures. Eur J Environ Civ Eng 2010;14(4):441–66.
[32] Ha T-H, Muralidharan S, Bae J-H, Ha Y-C, Lee H-G, Park K-W, et al. Accelerated short-term techniques to evaluate the corrosion performance of steel in fly ash blended concrete. Build Environ 2007;42:78–85.
[33] Song H-W, Saraswathy V. Corrosion monitoring of reinforced concrete structures – a review. Int J Electrochem Sci 2007;2:1–28.
[34] Okeniyi JO, Obiajulu UE, Ogunsanwo AO, Odiase NW, Okeniyi ET. CH4 emission model from the waste of Sus Domesticus and Gallus Domesticus in Nigerian local farms: environmental implications and prospects. Mitig Adapt Strateg Glob Chang 2013;18(3):325–35.
[35] Haynie FH. Statistical treatment of data, data interpretation, and reliability. In: Baboian R, editor. Corrosion tests and standards – application and interpretation. West Conshohocken, PA: ASTM International; 2005. p. 83–8.
[36] Soong TT. Fundamentals of probability and statistics for engineers. England: John Wiley & Sons Ltd; 2004.
[37] Ajayi OO, Fagbenle RO, Katende J, Okeniyi JO. Availability of wind energy resource potential for power generation at Jos, Nigeria. Front Energy 2011;5(4):376–85.
[38] Ajayi OO, Fagbenle RO, Katende J, Okeniyi JO, Omotosho OA. Wind energy potential for power generation of a local site in Gusau, Nigeria. Int J Energy Clean Environ 2011;11(1–4):99–116.
[39] Murthy DNP, Xie M, Jiang R. Weibull models. Hoboken, New Jersey: John Wiley & Sons, Inc; 2004.
[40] Montgomery DC, Runger GC. Applied statistics and probability for engineers. 3rd ed. New York: John Wiley & Sons Inc.; 2003.
[41] Fagbenle RO, Katende J, Ajayi OO, Okeniyi JO. Assessment of wind energy potential of two sites in North–East, Nigeria. Renew Energy 2011;36:1277–83.
[42] Thas O. Comparing distributions. New York: Springer Science+Business Media, LLC.; 2010.
[43] Izquierdo D, Alonso C, Andrade C, Castellote M. Potentiostatic determination of chloride threshold values for rebar depassivation: experimental and statistical study. Electrochim Acta 2004;49:2731–9.
[44] Roberge PR. Statistical interpretation of corrosion test results. In: Covino Jr, Bernard S, Cramer SD, editors. Corrosion: Fundamentals, Testing, and Protection, ASM Handbook, Vol. 13A, ASM, International; 2003. p. 425–429.
[45] Roberge PR. Handbook of corrosion engineering. New York: McGraw-Hill Companies, Inc; 2000.
[46] Kuang F, Zhang J, Zou C, Shi T, Wang Y, Zhang S, et al. Electrochemical methods for corrosion monitoring: a survey of recent patents. Recent Pat Corros Sci 2010;2:34–9.
[47] Afolabi AS, Alaneme KK, Bada SO. Corrosion behavior of austenitic and duplex stainless steels in lithium bromide. Leonardo Electron J Pr Technol 2009;14:1–10.